**Supplementary Figure S1. (A)** Pedigrees of experimental samples. The samples were named according to the following conventions. "**L**" indicates that the cells were growing **L**ogarithmically when harvested. "**S**" means that the cells were in **S**tationary phase when harvested. "**F**" means that the cells were **F**ixed with formaldehyde prior to harvesting, while "**U**" indicates that the cells were **U**nfixed when harvested. "**B**" indicates that the band excised from the prep gel was **B**roader than usual and thus contained a wider range of fragment sizes, while "**N**" means the excised band was relatively **N**arrow, with the intention of analyzing primarily fragments close to mono-nucleosome size. The cells used in the LUN, LFB and LFN samples came from the same batch of log-phase cells, while the cells used in the SUN sample came from an independent stationary-phase culture. For the LUN and SUN samples, the cells were not fixed with formaldehyde. **(B)** Conditional probability of nucleosome start at TSSs for all four of our samples over 2001-bp windows centered on transcriptional start sites (TSSs). **(C)** Profiles of MNase protection at TSSs for all four of our samples.
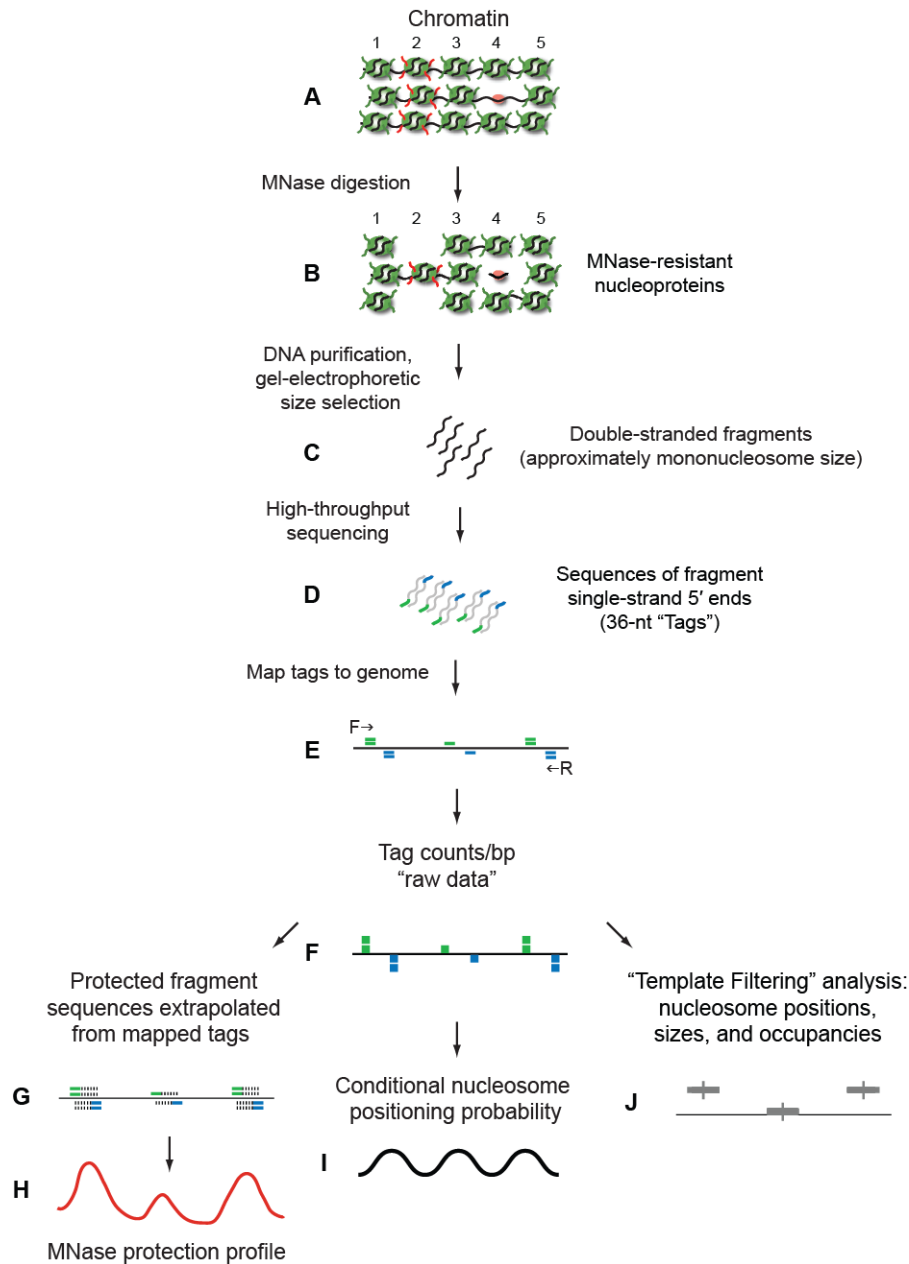
Supplementary Figure S2. Experimental design and data flow. (**A**) Chromatin structure may differ among cells in a population. Black line, DNA. Green ellipses, nucleosomes. Green and red lines, histone tails with differing modifications. Pink ellipse, a non-nucleosomal, DNA-binding protein complex. (**B**) Result of moderate digestion by Micrococcal Nuclease (MNase). (**C**) Double-stranded DNA fragments remaining after gel-electrophoretic selection of mono-nucleosome-sized DNA. (**D**) High-throughput sequencing (Illumina) yields 36 nucleotides of sequence information (a sequence "tag") from the 5′ end of the upper (green) and lower (blue) strand of each DNA fragment from panel **C**. (**E**) The sequence tags are mapped to the fission yeast genome. (**F**) The number of tags that start at each nucleotide position is counted. (**G**) Each tag is computer-extrapolated to a final length of 120 nt. (**H**) The number of times each nucleotide position is contained within a 120-bp extrapolated tag, regardless of strand, is counted. The number of counts at each position is then divided by the genome average for number of counts per position. The resulting numbers are plotted against nucleotide position to generate a "relative MNase-protection profile". (**I**) The raw data in panel F can also be used to calculate "conditional nucleosome positioning probability" (1). (**J**) As an alternative method for viewing nucleosome positions, sizes and occupancies, the "raw data" (tag counts in each strand at each position) from panel **F** are processed by the "template-filtering" algorithm of Weiner et al. (2). The results are represented graphically as horizontal bars centered on the position determined by the algorithm to be the center of that particular nucleosome (short vertical line). The width of each bar shows the algorithm-calculated size of each nucleosome, and the height of each bar is proportional to the average of the separately-calculated occupancies for the upper and lower strands of each nucleosome.
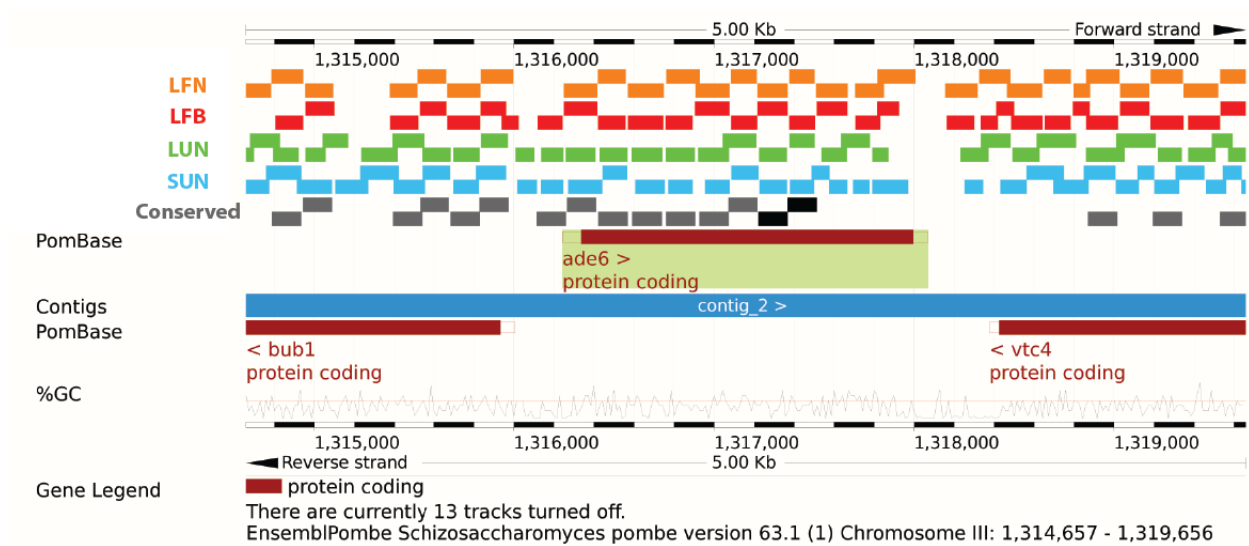
Supplementary Figure S3. Nucleosomes called by template filtering (2) are graphically shown using the Ensembl interface hosted by PomBase (http://www.pombase.org/). Log fixed narrow (LFN - orange), Log fixed broad (LFB – red), Log unfixed narrow (LUN – green), and Stationary unfixed narrow (SUN – blue) are shown in a 5kb window around the ADE6 gene. Conserved nucleosomes are displayed as lenient (grey) and stringent (black).

A

B
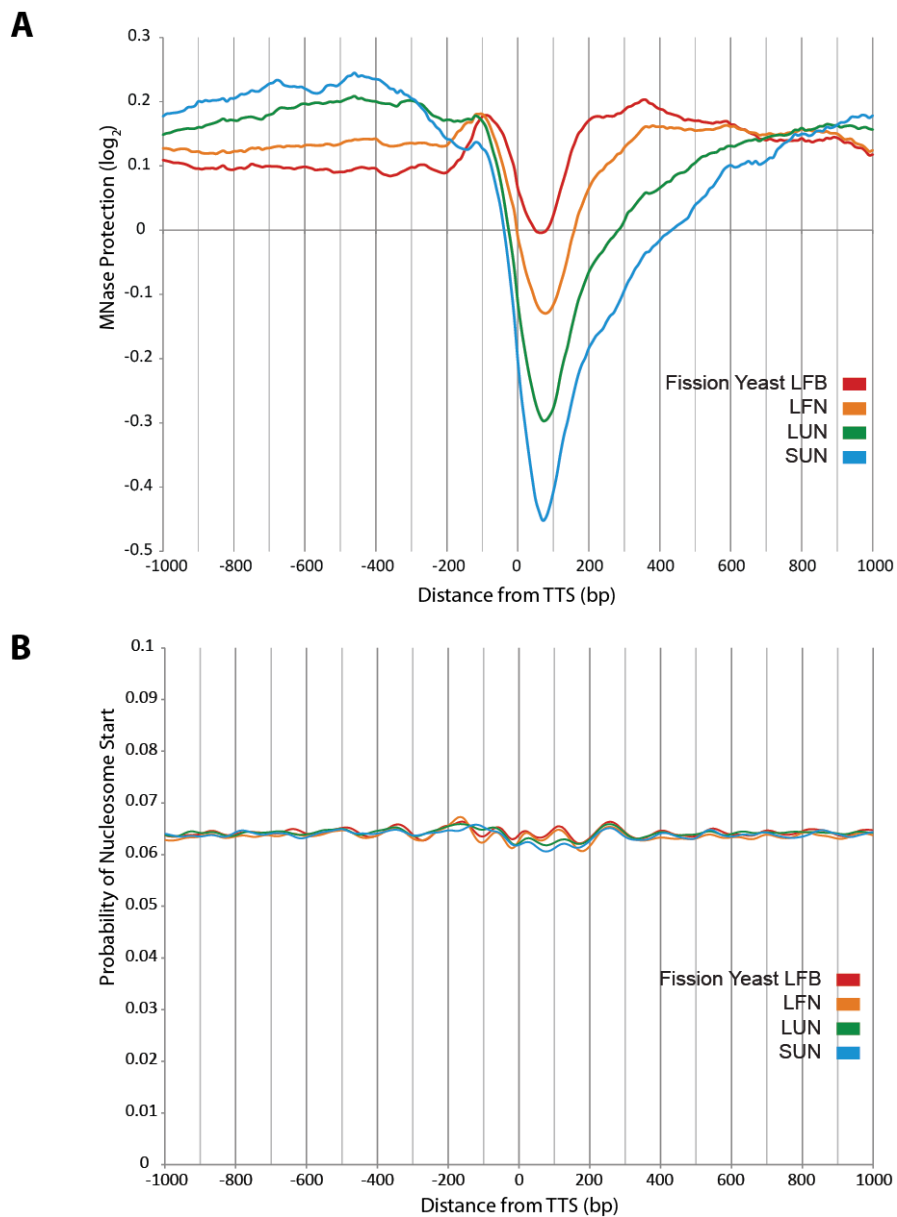
Supplementary Figure S4. **(A)** Profiles of MNase protection over 2001-bp windows centered on transcriptional termination sites (TTSs) for our four samples. **(B)** Conditional probability of nucleosome start at TTSs.
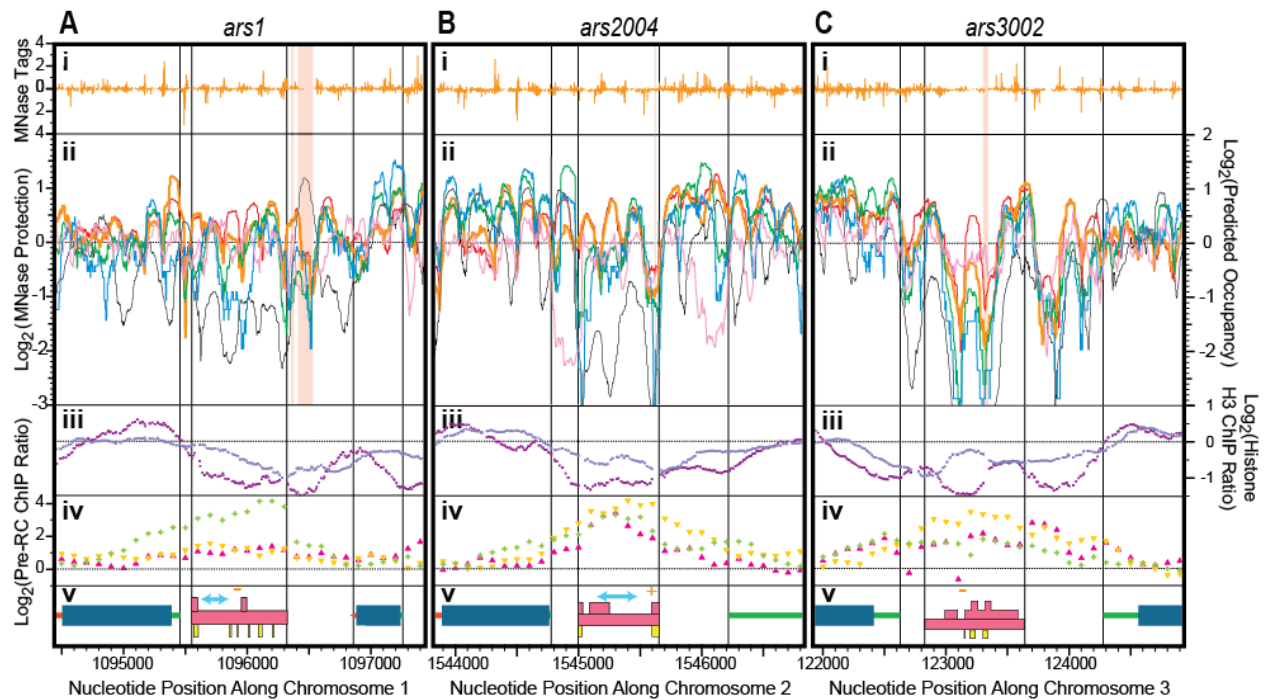
Supplementary Figure S5. Chromatin Structures of Three Well-Studied Replication Origins. Each vertical panel shows 3 kbp surrounding (**A**) *ars1,* (**B**) *ars2004,* (**C**) *ars3002.* Panels (i): (orange lines, ▌) number of MNase sequence tags per million in the LFN sample. Tags mapping to the top (bottom) strand are shown above (below) the 0 line. Panels (ii): MNase protection relative to genome average, LFN sample (orange line ▌); LFB sample (red line ▌); LUN sample (green line ▌); SUN sample (blue line ▌); data of Lantermann et al. (3) (pink line ▐). Pale pink-orange vertical bars (▐): regions of reduced mappability due to sequence repetitions. Black line, ▌: predicted nucleosome occupancy, based on algorithm of Kaplan et al. (4), right-hand scale. Panels (iii): ChIP-chip signal ratios relative to genome average for histone H3. Data from Buchanan et al. ((5); blue-gray line, ▌) and Durand-Dubief et al. ((6); purple line, ▌). Panels (iv): ChIP-chip signal ratios (log₂) for ORC1 (magenta triangles, ▲), ORC4 (inverted yellow triangles, ▼), and MCM6 (yellow-green crosses, +). Data from Hayashi et al. (7). Panels (v): coding regions (thick blue bars, ▬), 5′-UTRs (thin green bars, —), and 3′-UTRs (thin red bars, —) of the genes flanking the depicted origins. Pink boxes, ▬: regions defined genetically as important for ARS activity; upper boxes show small especially important regions. Lower, yellow boxes, ▐: *in vitro* ORC binding sites. Small orange minus (-) and plus (+) signs: positions of origin centers and orientations according to ArchAlign (8). Double-headed light cyan arrows in (**A**v) and (**B**v), ↔: positions from which replication forks diverge (9,10). Thin black vertical guide lines: boundaries of TSSs, TTSs and genetically-defined origins. See the main text for details.
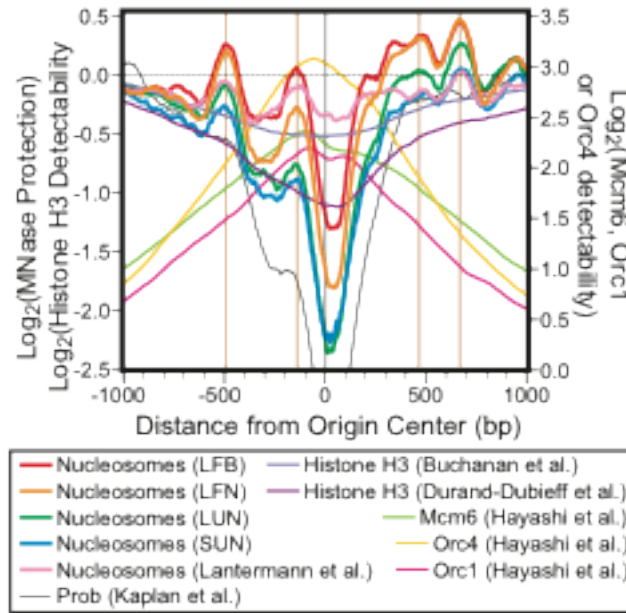
Supplementary Figure S6. Average distribution profiles of MNase protection, histone H3, and pre-RC proteins around 217 replication origins aligned by ArchAlign software. Average MNase protection around replication origins after alignment with ArchAlign, LFN sample (orange line ▌); LFB sample (red line ▌); LUN sample (green line ▌); SUN sample (blue line ▌); data of Lantermann et al. (3) (pink line ▌). Black line, ▌: predicted nucleosome occupancy, based on algorithm of Kaplan et al. (4). Average signal ratios for histone H3. Data from Buchanan et al. ((5); blue-gray line, ▌) and Durand-Dubief et al. ((6); purple line, ▌). Average ChIP-chip signal ratios (log$_2$) for ORC1 (magenta line, ▌), ORC4 (yellow line, ▌), and MCM6 (yellow-green crosses, ▌). Data from Hayashi et al. (7).
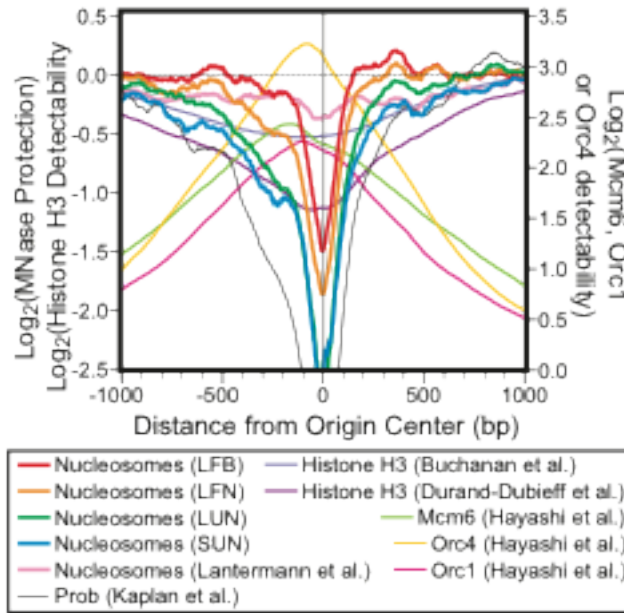
Supplementary Figure S7. Average distribution profiles of MNase protection, histone H3, and pre-RC proteins around 217 replication origins aligned by eye. Average MNase protection around replication origins after alignment with ArchAlign. LFN sample (orange line ▌); LFB sample (red line ▌); LUN sample (green line ▌); SUN sample (blue line ▌); data of Lantermann et al. (3) (pink line ▌). Black line, ▌: predicted nucleosome occupancy, based on algorithm of Kaplan et al. (4). Average signal ratios for histone H3. Data from Buchanan et al. (5); blue-gray line, ▌) and Durand-Dubief et al. ((6); purple line, ▌). Average ChIP-chip signal ratios (log$_2$) for ORC1 (magenta line, ▌), ORC4 (yellow line, ▌), and MCM6 (yellow-green crosses, ▌). Data from Hayashi et al. (7).

References for Supplementary Figures

1. Kaplan, N., Hughes, T.R., Lieb, J.D. and Segal, E. (2010) Contribution of histone sequence preferences to nucleosome organization: proposed definitions and methodology. *Genome Biology*, **11**, 140.
2. Weiner, A., Hughes, A., Yassour, M., Rando, O.J. and Friedman, N. (2010) High-resolution nucleosome mapping reveals transcription-dependent promoter packaging. *Genome Research*, **20**, 90-100.
3. Lantermann, A.B., Straub, T., Strålfors, A., Yuan, G.-C., Ekwall, K. and Korber, P. (2010) *Schizosaccharomyces pombe* genome-wide nucleosome mapping reveals positioning mechanisms distinct from those of *Saccharomyces cerevisiae*. *Nat Struct Mol Biol*, **17**, 251-257.
4. Kaplan, N., Moore, I.K., Fondufe-Mittendorf, Y., Gossett, A.J., Tillo, D., Field, Y., LeProust, E.M., Hughes, T.R., Lieb, J.D., Widom, J. *et al.* (2009) The DNA-encoded nucleosome organization of a eukaryotic genome. *Nature*, **458**, 362-366.
5. Buchanan, L., Durand-Dubief, M., Roguev, A., Sakalar, C., Wilhelm, B., Strålfors, A., Shevchenko, A., Aasland, R., Shevchenko, A., Ekwall, K. *et al.* (2009) The *Schizosaccharomyces pombe* JmjC-protein, Msc1, prevents H2A.Z localization in centromeric and subtelomeric chromatin domains. *PLoS Genet*, **5**, e1000726.
6. Durand-Dubief, M., Persson, J., Norman, U., Hartsuiker, E. and Ekwall, K. (2010) Topoisomerase I regulates open chromatin and controls gene expression *in vivo*. *EMBO J*, **29**, 2126-2134.
7. Hayashi, M., Katou, Y., Itoh, T., Tazumi, A., Yamada, Y., Takahashi, T., Nakagawa, T., Shirahige, K. and Masukata, H. (2007) Genome-wide localization of pre-RC sites and identification of replication origins in fission yeast. *EMBO J*, **26**, 1327-1339.
8. Lai, W. and Buck, M.J. (2010) ArchAlign: Coordinate-free chromatin alignment reveals novel architectures. *Genome Biology*, **11**, R126.
9. Gomez, M. and Antequera, F. (1999) Organization of DNA replication origins in the fission yeast genome. *EMBO J.*, **18**, 5683-5690.
10. Okuno, Y., Okazaki, T. and Masukata, H. (1997) Identification of a predominant replication origin in fission yeast. *Nucleic Acids Res.*, **25**, 530-536.